Cronfa - Swansea University Open Access Repository

_____

This is an author produced version of a paper published in:
ACS Energy Letters

_____

Cronfa URL for this paper:
http://cronfa.swan.ac.uk/Record/cronfa34445

_____

Paper:

Pockett, A. & Carnie, M. (2017). Ionic Influences on Recombination in Perovskite Solar Cells. *ACS Energy Letters*
http://dx.doi.org/10.1021/acsenergylett.7b00490

_____

LETTER

Ionic Influences on Recombination in Perovskite Solar Cells

Adam Pockett[ID] and Matthew J. Carnie*[ID]

Materials Research Centre, College of Engineering, SPECIFIC—Swansea University, Bay Campus, Swansea SA1 8EN, United Kingdom

ⓢ *Supporting Information*

ABSTRACT: The origins of recombination processes, particularly those that relate to current−voltage hysteresis, are still unclear in perovskite solar cells. Of particular interest is the impact different contact materials have on the level of hysteresis observed. This work shows that there is a clear link between ionic movement and interfacial recombination, which have both been shown to be responsible for hysteresis. When low-temperature transient photovoltage (TPV) measurements are performed over a period in which ions redistribute within the perovskite layer, the dominant recombination mechanism, responsible for hysteresis and other slow dynamic processes, is found to occur at the TiO_2/perovskite interface. We observe an anomalous negative transient upon firing the laser pulse, which we attribute to interfacial recombination at the TiO_2/perovskite interface. The impact of recombination at the perovskite/ HTL interface is shown to be negligible by performing TPV measurements using different laser wavelengths to probe different depths into the perovskite layer, as well as by changing the type of HTL used.
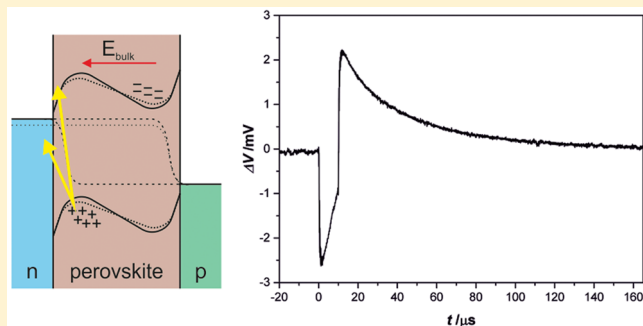
The number of publications concerning organic−inorganic metal trihalide perovskite solar cells has grown exponentially since the publication of two breakthrough papers demonstrating high efficiency solid-state devices in 2012.[1,2] While silicon photovoltaic (PV) modules have decreased in cost during this period,[3] perovskite materials will have applications where silicon PV alone may not be suitable, such as for indoor applications[4] and in tandem multijunction solar cells.[5,6] Silicon solar cells also have higher embodied energies due to the high-temperature manufacturing processes involved, whereas perovskite devices can be fabricated using low-temperature methods.[7,8]

One of the key curiosities encountered in the field is the hysteresis exhibited in the current−voltage ($I-V$) curves of perovskite devices. Surface defect densities, ferroelectric effects, and mobile ions were all offered as possible explanations for the observed differences, whereby efficiencies obtained when scanning in the V_{oc} to I_{sc} direction are higher than those in the I_{sc} to V_{oc} direction.[9] The history of the device prior to the $I-V$ sweep significantly influences the $I-V$ characteristics and therefore the calculated efficiency. It was shown that preconditioning the device, by light soaking and/or holding at forward bias, gave more favorable $I-V$ characteristics.[10] This suggested that some form of polarization effect could be taking place and that the nature of this could be mobile ions accumulating at carrier-selective interfaces.[11] Indeed, drift−diffusion models are able to recreate the $I-V$ hysteresis effect

when buildup of ionic charge at interfaces is taken into account.[12,13] Iodide diffusion,[14] methylammonium diffusion,[15] and proton diffusion[16] have been postulated as being responsible for the observed hysteresis, but as Frost and Walsh have pointed out, the response is most likely a combination of several processes. They do, however, state that fast vacancy-mediated anion diffusion is the dominant process in methylammonium and formamidinium lead trihalide perovskite materials.[17]

If we accept that ion migration is the major factor causing hysteresis and that computational models do support the hypothesis, further measurements are required to add weight to the evidence. Attempts have been made to measure this directly using time-of-flight secondary-ion mass spectrometry (TOF-SIMS)[18] or glow discharge optical emission spectrometry (GD-OES).[19] Ion migration can also be observed indirectly, for example temperature-dependent measurements have been used to calculate activation energies for the underlying processes behind hysteresis.[14,20]

In this work, we demonstrate the influence of different contact materials on ion migration and recombination within perovskite solar cells using transient photovoltage (TPV) decay measurements. Using low-temperature measurements, we show

that light-induced polarization of perovskite devices occurs and that anomalies in the TPV decay traces can be explained via the build-up and discharge of mobile ions affecting interfacial recombination processes, predominantly at the TiO_2/perovskite interface. We will also show evidence that there is perhaps more than one mobile species.

TPV measurements are widely used to study recombination lifetimes in a range of solar cell technologies,[21−23] and we have previously demonstrated TPV's usefulness in characterizing perovskite solar cells.[24−26] In the case of perovskite solar cells it has been shown that the time constant obtained from TPV measurements can be related to the dominant recombination mechanism within the device.[27] Recombination in perovskite devices has also been studied extensively using techniques including impedance spectroscopy (EIS),[28,29] intensity modulated photovoltage/photocurrent spectroscopy (IMVS/IMPS),[30,31] and open-circuit photovoltage decay (OCVD).[32−34] It has been demonstrated by these techniques that there are several processes occurring within the devices which often leads to a complex response from which it is difficult to deconvolve individual processes. In particular, many perovskite devices display a slow dynamic response which is most commonly observed as hysteresis in the $I-V$ curve. This slower component is also observed in EIS, IMVS, and OCVD measurements.[20]

Modeling and experimental results have shown that hysteresis (and associated slow dynamic processes) is linked to ion migration within the perovskite layer and the impact these ions have on recombination at the interfaces with charge-selective contacts.[13,20,33,35] A particularly interesting observation is the slow rise in open-circuit voltage, from a dark equilibrium starting condition, upon illumination. This suggests an initial high rate of recombination, which leads to a suppression of the measured V_{oc}. The slow increase to a steady-state V_{oc} has been shown to be linked to ionic movement and suggests that the rate of recombination is reduced as ions migrate.[20,33] The issue with many time and frequency domain electrical characterization techniques is that they often rely on the device being at a steady state. This usually requires waiting for several minutes until a stable V_{oc} has been reached under illumination. This makes the initial response, with high rates of recombination, difficult to probe with conventional approaches.

An adapted TPV technique developed by Calado et al. has shown that the recombination processes occurring within a device change over time as the V_{oc} rises (ions redistribute).[36] This method involves performing multiple TPV measurements during the slow V_{oc} rise due to turning on the background illumination. Because each TPV transient measurement takes only a few hundreds of microseconds, compared to the slow V_{oc} rise having a time constant on the order of seconds, the ionic distribution can be thought of as being fixed during the transient. Calado et al. observed a negative photovoltage deflection in response to a laser pulse at short times (low V_{oc}). As the V_{oc} rose, the extent of the negative response was reduced until the transient became purely positive as the V_{oc} approached the steady-state condition.[36] Simulations of the observed transient behavior indicated that there were high rates of interfacial recombination occurring when the device was not at steady state. It was not conclusive whether this recombination was dominant at a single interface, or if it was present at both contacts.

We have modified this "transients of the transient" technique by conducting the experiments at low temperatures, slowing the redistribution of ions further, in order to study the impact of different contact materials on recombination within planar perovskite devices. Of particular interest is the origin of hysteresis in cells based on a compact TiO_2 (c-TiO_2) electron transport layer (ETL). Hysteresis and the slow rise in V_{oc} is frequently observed in these cells and is not observed at room temperature in cells with an inverted architecture using phenyl-C61-butyric acid methyl ester (PCBM).[37] However, these inverted cells also use poly(3,4-ethylenedioxythiophene) polystyrenesulfonate (PEDOT:PSS) as the hole transport layer (HTL), as opposed to Spiro-OMeTAD in the case of the c-TiO_2 cells. Therefore, it is not immediately clear if the reduction in these observable slow processes is due to the change in ETL alone.

To investigate this, both c-TiO_2/Spiro and PCBM/PEDOT contact cells are studied here, as well as cells in which the Spiro-OMeTAD is replaced by "undoped" P3HT. The perovskite layer deposition method was kept consistent for all devices in an attempt to allow a fair comparison (see the Supporting Information for experimental methods). Table 1 lists the

Table 1. Photovoltaic Parameters of Cells Tested in This Study, Measured under AM1.5 1 Sun Illumination[a]

cell	scan dir.	J_{sc} (mA cm^{-2})	V_{oc} (V)	FF (%)	PCE (%)
TiO$_2$/Spiro	rev	21.5	1.05	56.0	12.7 (11.2 ± 1.2)
	for	20.8	1.03	25.1	5.4 (4.8 ± 0.4)
PCBM	rev	20.0	0.97	64.9	12.6 (12.1 ± 0.3)
	for	19.5	0.97	63.7	12.0 (11.9 ± 0.3)
TiO$_2$/P3HT	rev	15.5	1.10	45.0	7.7 (6.5 ± 1.2)
	for	15.0	1.00	14.5	2.2 (3.0 ± 1.0)

[a]Values are for champion cell performance. Values in parentheses are average values ± standard deviation for the batches of cells (minimum of 6 cells for each architecture).

photovoltaic performance parameters for the devices tested in this study (see the Supporting Information for $I-V$ curves). The cells are representative of other devices with similar architectures in the literature, although the fabrication method was not optimized for the P3HT devices. The level of hysteresis between the reverse (forward bias to short-circuit) and forward (short-circuit to forward bias) scan directions is significantly lower in the organic contact PCBM/PEDOT:PSS cells compared to those employing c-TiO_2 as the ETL. The degree of hysteresis between the Spiro and P3HT cells is comparable.

Multiple processes are often seen in perovskite TPV measurements in the form of biexponential photovoltage decays.[25,27,38] The faster of the two decay time constants has been attributed to the predominant charge recombination pathway in the device and can be used to reconstruct the $I-V$ curve.[27] The slower component is observed in cells with incomplete perovskite coverage and has been related to recombination at the unintentional interface between TiO_2 and Spiro.[38] All cells studied in this work displayed purely monoexponential decay behavior suggesting that the perovskite films are of high quality, as is consistent with the solvent dripping technique employed during the perovskite layer deposition.[39]

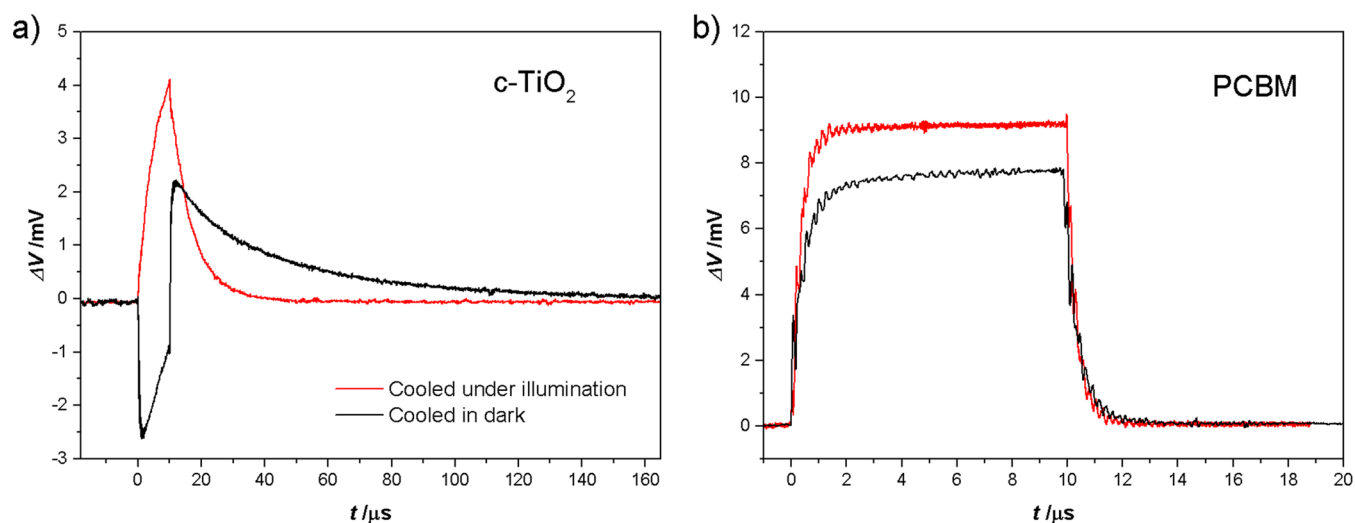As the slow V_{oc} rise is governed by the movement of ionic species within the perovskite, its rate is highly temperature-

Figure 1. TPV measurements for c-TiO$_2$ (a) and PCBM (b) based devices at 223 K cooled under illumination and in the dark. Laser pulse length of 10 μs; LED bias illumination equivalent to 1 Sun was used.
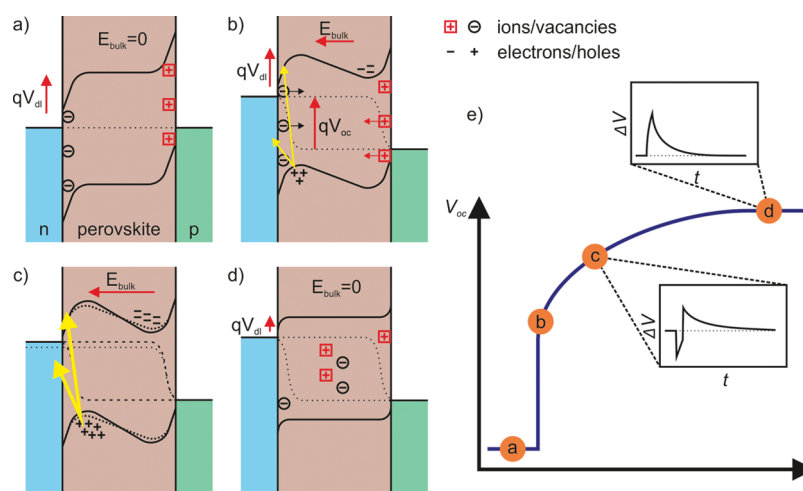

Figure 2. Schematic of band structure under different conditions. (a) Equilibrium in the dark: built-in voltage screened by the formation of ionic double layers at the interfaces. (b) Initial response to illumination: charge accumulation in potential valleys near opposing selective contacts, interfacial recombination (yellow arrows) suppresses V_{oc}, double layers begin to discharge. (c) Response to laser pulse: increase in carrier density in potential valleys near interfaces leads to increase in recombination rate (observed negative voltage transient). (d) Steady state: double layers discharged (cooled under illumination state). (e) Schematic showing slow V_{oc} rise and position of steps a–d.

dependent. In order to increase the time available for studying the initial recombination behavior, as the ions redistribute, the TPV measurements were carried out at low temperature. The cells were kept in the dark at room temperature to allow them to reach equilibrium. The temperature was then reduced to 223 K, before turning on the white bias light (1 Sun equivalent intensity) and initiating the laser pulses (see the Supporting Information for a schematic of the measurement procedure).

The response for a c-TiO$_2$/Spiro cell during the slow voltage rise (V_{oc} = 0.94 V) is shown in Figure 1a. This shows a fast negative response to the laser pulse at t = 0. The reduction in voltage occurs on a time scale beyond the resolution of the measurement system. During the 10 μs laser pulse, the voltage recovers slightly. As the laser pulse is extinguished, the voltage immediately recovers and becomes positive. The voltage then decays more slowly back to the steady-state value.

To show that this behavior is not a consequence of the low-temperature measurement, the device was also cooled to 223 K under illumination (V_{oc} allowed to reach steady state before

cooling). A negative voltage response is not observed, and the transient is comparable to that at room temperature. In the case of cooling under illumination, the cells V_{oc} increases slightly to around 1.07 V from the initial room-temperature steady state of 1.04 V.

Figure 1b shows the transient photovoltage response from a low hysteresis PCBM/PEDOT contact cell under the same measurement procedure. A negative transient is not observed for this cell architecture from either cooling in the dark or under illumination. This is consistent with the faster voltage response to illumination in these cells. Even when illuminated from a dark equilibrium condition at 223 K, the V_{oc} stabilizes to a steady-state value around 0.99 V in less than 1 s.

A number of studies have shown that while PCBM-based cells show no apparent hysteresis at room temperature, at lower temperatures some hysteretic behavior is observed.[36,37] This behavior is not apparent in the TPV measurements shown here. Ionic movement in the bulk of the perovskite is likely to be relatively unaffected by the difference in contact materials used

here. This suggests that the presence or absence of hysteresis and other slow responses is due to interfacial processes in conjunction with the ionic distribution. As shown in previous work, the calculated concentration of iodide vacancies within the perovskite is sufficient to form double layers at the contacts which act to screen the built-in field (Figure 2a).[20] The built-in field is reduced under illumination because of the splitting of the Fermi levels. At open-circuit under 1 Sun illumination, a V_{oc} of around 1 V is expected. The double layers will therefore discharge (ions will diffuse back into the bulk). It is this notable change in ionic distribution near the interfaces that impacts significantly on recombination in that region.

As illustrated in Figure 2, the electronic band structure of the device is likely to be quite different depending on the preconditioning before the transient measurement is performed.

In the case of the measurement performed on the cell with a dark starting condition, an electric field opposing the normal direction of carrier transport will exist until the ions have had time to discharge from the interfacial double layers to compensate for the response to the background illumination (Figure 2b). This electric field results in accumulation of electrons and holes near their respective blocking contacts. High rates of recombination can be expected in these regions because of the high carrier concentrations. The additional laser pulse will increase the magnitude of the unfavorable electric field, increasing the carrier accumulation in the regions of high rates of recombination (Figure 2c). This will further increase the rate of recombination, leading to the negative voltage spike when the laser is switched on. The photovoltage is able to recover during the laser pulse as the increased charge accumulation shields the potential valleys near the contacts. When the laser pulse is switched off, the associated increase in interfacial recombination will quickly diminish resulting in the positive voltage recovery.

In the case of the device being preilluminated (already at steady state), the double layers are likely to be completely discharged, so that when the Fermi level splitting is perturbed by the laser pulse potential valleys near the interface are not created (Figure 2d). The absence of the negative photovoltage transient in this condition therefore relates to the absence of these regions of high charge accumulation near the interfaces.

Numerous literature reports using measurements performed near steady state have shown that the main recombination process occurring in perovskite devices is in the bulk.[40−42] The results presented here do not contradict this evidence, as shown by the fact that the steady-state V_{oc} is similar for all devices, i.e. bulk recombination is not affected by contact properties. The negative TPV transient is evidence that during the initial response to illumination there is an additional high rate of interfacial recombination occurring at the TiO$_2$/perovskite interface which leads to very different V_{oc} values relative to PCBM devices at short times.

As the TPV results are believed to be evidence of recombination occurring close to the interface, the measurements were also performed using different wavelength lasers to alter the light penetration depth and therefore the region being probed. The background illumination was provided by a white LED to provide a homogeneous carrier generation profile throughout the devices' active layer. The small perturbation provided by the laser pulse generates a small excess of free carriers in different regions of the perovskite layer depending on the wavelength used. At 405 nm, the penetration depth is

around 50 nm assuming an absorption coefficient of 2×10^5 cm^{-1}.[43] Therefore, using this short wavelength laser should predominantly probe the recombination processes occurring near the TiO$_2$ interface, rather than in the bulk. The use of green and red lasers provides more homogeneous excitation throughout the bulk of the device. There was no qualitative difference between the transient responses for any of the 3 different wavelengths used (see the Supporting Information). Because excitation at each of the wavelengths increases carrier generation close to the interface with TiO$_2$, but in the case of the 405 nm laser not necessarily in the bulk, it can be concluded that the consistent response is evidence that the main recombination pathway responsible for the negative transient is occurring in the region near the TiO$_2$ contact. The fact that the blue laser induces the negative transient response, being indicative of high rates of recombination, suggests that the enhanced recombination is not occurring at the perovskite/HTL interface as short wavelength light does not penetrate far enough into the device to generate carriers near that contact.

The progression of the transient response over several minutes during the slow voltage rise is shown in Figure 3
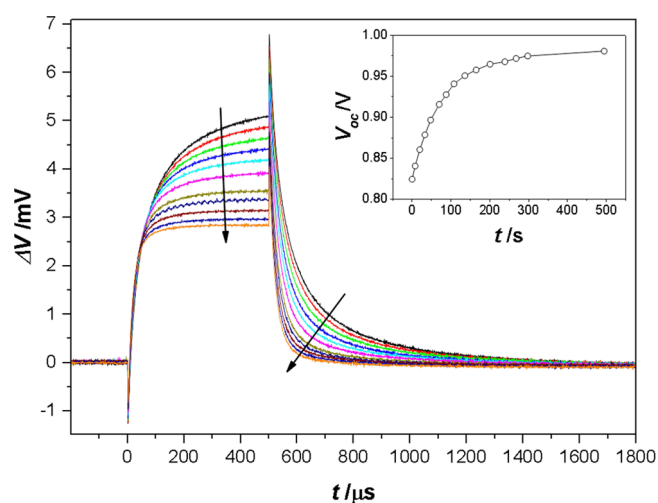

Figure 3. Progression of the transient measurements over time for the c-TiO$_2$ device, cooled to 223 K in the dark. Inset: open-circuit voltage rise during transient measurements.

(inset: slow V_{oc} rise). In this instance, the laser pulse length was set to 500 μs to allow the voltage to fully recover after the initial negative spike. During the voltage rise the transient rise and decay behavior is consistent with an increase in carrier concentration, i.e. for a higher V_{oc}, decay lifetime is reduced. After 500 s from initially turning on the bias light, the V_{oc} has risen to 0.98 V, which is close to the steady-state V_{oc} of approximately 1 V. However, the voltage spikes in response to the laser being turned on and off are still present, although reduced slightly in magnitude.

After 1 h of illumination the cells' V_{oc} reaches a steady state at 1 V. Interestingly, the voltage spikes associated with the laser switch on and off points are still present even though the background V_{oc} has reached the same steady-state level as when the device is preconditioned under illumination before cooling, as displayed in Figure 4. The spikes do not appear in the transients for the preilluminated condition. The amplitude of the spikes has decreased to around 50% of the initial value, indicating that the recombination process associated with them
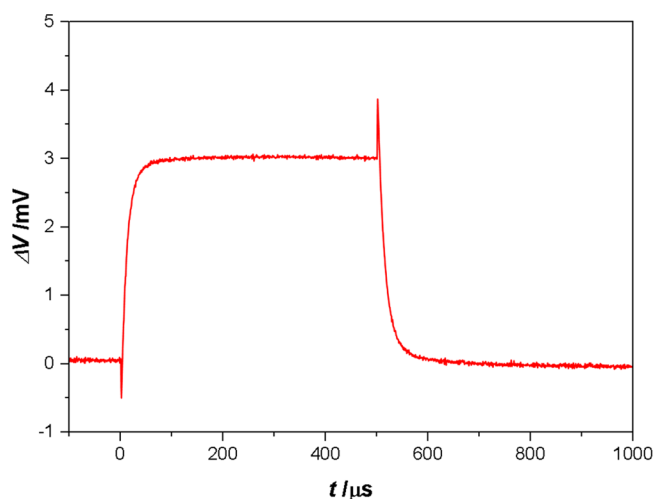
Figure 4. Transient response at 223 K after 1 h illumination from dark starting condition.
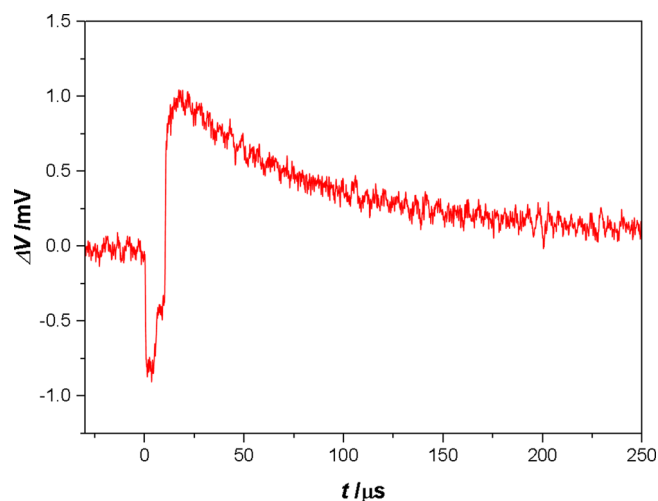

Figure 5. Transient response of P3HT-based solar cell after being cooled to 223 K in the dark.

is being reduced very slowly. If the sample is allowed to warm up to room temperature the spikes decrease at a faster rate. Again, this is consistent with the recombination process being screened by ionic movement. However, because the V_{oc} rise is much faster than the fading of the spikes, it suggests that there is more than one process involved.

This could involve the movement of two different ionic species at different rates, or perhaps a single species in different environments. A range of studies have indicated that iodide ions are able to easily diffuse through the perovskite lattice.[14,15,44] Methylammonium ions are also thought to be mobile, albeit with a lower diffusion coefficient due to restrictions relating to the rotation of the cation and its ability to pass through the lead iodide lattice.[14] The slow process could therefore be related to the migration of methylammonium ions.

If the observations were caused by a single ion species, most likely iodide, then the presence of multiple processes could be due to iodide migration via grain boundaries and through the bulk. It has been shown that iodide migration along grain boundaries is much faster than through the bulk.[45] Alternatively, the faster of the two processes may relate to the discharge of the ionic double layers, whereas the slower process may be due to iodide ions that are immobilized at the TiO_2 surface. The interaction between TiO_2 and iodide has been shown to have significant effects on the electronic band structure.[46] There is also the possibility that ions added as "dopants" to the Spiro HTL may diffuse through the perovskite. For example, lithium ions are likely to be highly mobile because of their small radii. Li^+ ions are also known to strongly interact with TiO_2, which could alter transport and recombination mechanisms at that interface.[18,47] To test if the observations made here are related to the Spiro-OMeTAD layer, or more specifically its additives, we fabricated devices in which "undoped" P3HT was used as the HTL. The TPV response from a cell containing c-TiO_2/P3HT contacts, without additives, is comparable to that for the Spiro cell, as shown in Figure 5. This indicates that the dominant recombination process responsible for the observed slow dynamic behavior and negative transients is occurring at the TiO_2 interface. This also suggests that the reduction in hysteresis seen for inverted organic contact devices is due to

the replacement of the TiO_2 with PCBM, and that the PEDOT:PSS has a negligible impact.

These results clearly indicate that the main recombination process responsible for a variety of slow dynamic processes is occurring at or near the TiO_2/perovskite interface. This supports the assumptions made in drift–diffusion models that strong interfacial recombination is present in cells containing TiO_2.[13,36] The exact mechanism remains unclear, but it is clearly influenced by the ionic environment in that region. Yang et al. have shown using transient reflection spectroscopy that surface recombination limits the carrier lifetime in polycrystalline perovskite thin films.[48] This recombination appears to be passivated by the presence of PCBM at the interface, as no negative transient has been observed despite there likely being a similar electronic band structure to the TiO_2 devices as the ions will still be mobile. It is unclear as to whether the ions are directly promoting recombination, or if they are simply acting to modify the band structure. The presence of the ionic double layers at equilibrium results in the formation of potential valleys when initially illuminated. This results in the accumulation of a high concentration of holes near the TiO_2 interface which may quickly recombine with electrons possibly trapped at the surface of the TiO_2 or perovskite.[13,49] If this indeed was related to trapped electrons, it would suggest that they are either not present in PCBM, or that PCBM is able to passivate traps in the perovskite.[50]

In conclusion, we have shown that the dominant recombination mechanism responsible for the observed hysteresis in perovskite solar cells is occurring at or near the interface with the TiO_2 selective contact. Low-temperature measurements enabled the progression of this recombination process to be observed over time as the ions migrated away from the interface in response to the change in electric field under illumination. We observed a long-lived negative transient effect which indicates that there may be more than one ionic species responsible for this behavior. Even though hysteresis might not be considered important in "real world" applications, we have shown that this technique can be used to study detrimental recombination processes which are otherwise hidden by other effects.

ASSOCIATED CONTENT

Ⓢ Supporting Information

The Supporting Information is available free of charge on the ACS Publications website at DOI: 10.1021/acsenergy-lett.7b00490.

> Experimental methods, I−V curves, and TPV measurements with different wavelength lasers (PDF)

AUTHOR INFORMATION

Corresponding Author

*E-mail: m.j.carnie@swansea.ac.uk. Tel: +44 1792 60 6489.

ORCID Ⓞ

Adam Pockett: 0000-0002-4747-9560

Matthew J. Carnie: 0000-0002-4232-1967

Notes

The authors declare no competing financial interest.

All data created during this research are openly available from the Swansea University data archive at https://doi.org/10.5281/zenodo.820588.

ACKNOWLEDGMENTS

REFERENCES

(1) Lee, M. M.; Teuscher, J.; Miyasaka, T.; Murakami, T. N.; Snaith, H. J. Efficient Hybrid Solar Cells Based on Meso-Superstructured Organometal Halide Perovskites. *Science* **2012**, *338*, 643−647.

(2) Kim, H.-S.; Lee, C.-R.; Im, J.-H.; Lee, K.-B.; Moehl, T.; Marchioro, A.; Moon, S.-J.; Humphry-Baker, R.; Yum, J.-H.; Moser, J. E.; et al. Lead Iodide Perovskite Sensitized All-Solid-State Submicron Thin Film Mesoscopic Solar Cell with Efficiency Exceeding 9%. *Sci. Rep.* **2012**, *2*, 591.

(3) Green, M. A. Commercial Progress and Challenges for Photovoltaics. *Nat. Energy* **2016**, *1*, 15015.

(4) Raifuku, I.; Ishikawa, Y.; Ito, S.; Uraoka, Y. Characteristics of Perovskite Solar Cells under Low-Illuminance Conditions. *J. Phys. Chem. C* **2016**, *120*, 18986−18990.

(5) Albrecht, S.; Saliba, M.; Correa Baena, J. P.; Lang, F.; Kegelmann, L.; Mews, M.; Steier, L.; Abate, A.; Rappich, J.; Korte, L.; et al. Monolithic Perovskite/Silicon-Heterojunction Tandem Solar Cells Processed at Low Temperature. *Energy Environ. Sci.* **2016**, *9*, 81−88.

(6) Bailie, C. D.; Christoforo, M. G.; Mailoa, J. P.; Bowring, A. R.; Unger, E. L.; Nguyen, W. H.; Burschka, J.; Pellet, N.; Lee, J. Z.; Grätzel, M.; et al. Semi-Transparent Perovskite Solar Cells for Tandems with Silicon and CIGS. *Energy Environ. Sci.* **2014**, *8*, 956−963.

(7) Ball, J. M.; Lee, M. M.; Hey, A.; Snaith, H. J. Low-Temperature Processed Mesosuperstructured to Thin-Film Perovskite Solar Cells. *Energy Environ. Sci.* **2013**, *6*, 1739−1743.

(8) Carnie, M. J.; Charbonneau, C.; Davies, M. L.; Troughton, J.; Watson, T. M.; Wojciechowski, K.; Snaith, H.; Worsley, D. A. A One-Step Low Temperature Processing Route for Organolead Halide Perovskite Solar Cells. *Chem. Commun.* **2013**, *49*, 7893−7895.

(9) Snaith, H. J.; Abate, A.; Ball, J. M.; Eperon, G. E.; Leijtens, T.; Noel, N. K.; Stranks, S. D.; Wang, J. T. W.; Wojciechowski, K.; Zhang, W. Anomalous Hysteresis in Perovskite Solar Cells. *J. Phys. Chem. Lett.* **2014**, *5*, 1511−1515.

(10) Unger, E. L.; Hoke, E. T.; Bailie, C. D.; Nguyen, W. H.; Bowring, A. R.; Heumüller, T.; Christoforo, M. G.; McGehee, M. D. Hysteresis and Transient Behavior in Current−Voltage Measurements of Hybrid-Perovskite Absorber Solar Cells. *Energy Environ. Sci.* **2014**, *7*, 3690−3698.

(11) Tress, W.; Marinova, N.; Moehl, T.; Zakeeruddin, S. M.; Nazeeruddin, M. K.; Grätzel, M. Understanding the Rate-Dependent J−V Hysteresis, Slow Time Component, and Aging in $CH_3NH_3PbI_3$ Perovskite Solar Cells: The Role of a Compensated Electric Field. *Energy Environ. Sci.* **2015**, *8*, 995−1004.

(12) Richardson, G.; O'Kane, S. E. J.; Niemann, R. G.; Peltola, T. A.; Foster, J. M.; Cameron, P. J.; Walker, A. B. Can Slow-Moving Ions Explain Hysteresis in the Current-Voltage Curves of Perovskite Solar Cells? *Energy Environ. Sci.* **2016**, *9*, 1476−1485.

(13) Van Reenen, S.; Kemerink, M.; Snaith, H. J. Modeling Anomalous Hysteresis in Perovskite Solar Cells. *J. Phys. Chem. Lett.* **2015**, *6*, 3808−3814.

(14) Eames, C.; Frost, J. M.; Barnes, P. R. F.; O'Regan, B. C.; Walsh, A.; Islam, M. S. Ionic Transport in Hybrid Lead Iodide Perovskite Solar Cells. *Nat. Commun.* **2015**, *6*, 7497.

(15) Azpiroz, J. M.; Mosconi, E.; Bisquert, J.; De Angelis, F. Defect Migration in Methylammonium Lead Iodide and Its Role in Perovskite Solar Cell Operation. *Energy Environ. Sci.* **2015**, *8*, 2118−2127.

(16) Egger, D. A.; Kronik, L.; Rappe, A. M. Theory of Hydrogen Migration in Organic-Inorganic Halide Perovskites. *Angew. Chem., Int. Ed.* **2015**, *54*, 12437−12441.

(17) Frost, J. M.; Walsh, A. What Is Moving in Hybrid Halide Perovskite Solar Cells? *Acc. Chem. Res.* **2016**, *49*, 528−535.

(18) Li, Z.; Xiao, C.; Yang, Y.; Harvey, S. P.; Kim, D.; Christians, J. A.; Yang, M.; Schulz, P.; Nanayakkara, S. U.; Jiang, C.-S.; et al. Extrinsic Ion Migration in Perovskite Solar Cells. *Energy Environ. Sci.* **2017**, *10*, 1234−1242.

(19) Lee, H.; Gaiaschi, S.; Chapon, P.; Marronnier, A.; Lee, H.; Vanel, J.-C.; Tondelier, D.; Boureé, J.-E.; Bonnassieux, Y.; Geffroy, B. Direct Experimental Evidence of Halide Ionic Migration under Bias in $CH_3NH_3PbI_{3-x}Cl_x$ Based Perovskite Solar Cells Using GD-OES Analysis. *ACS Energy Lett.* **2017**, *2*, 943−949.

(20) Pockett, A.; Eperon, G. E.; Sakai, N.; Snaith, H. J.; Peter, L. M.; Cameron, P. J. Microseconds, Milliseconds and Seconds: Deconvoluting the Dynamic Behaviour of Planar Perovskite Solar Cells. *Phys. Chem. Chem. Phys.* **2017**, *19*, 5959−5970.

(21) Carnie, M. J.; Charbonneau, C.; Barnes, P. R. F.; Davies, M. L.; Mabbett, I.; Watson, T. M.; O'Regan, B. C.; Worsley, D. A. Ultra-Fast Sintered TiO_2 Films in Dye-Sensitized Solar Cells: Phase Variation, Electron Transport and Recombination. *J. Mater. Chem. A* **2013**, *1*, 2225−2230.

(22) Barnes, P. R. F.; Miettunen, K.; Li, X.; Anderson, A. Y.; Bessho, T.; Gratzel, M.; O'Regan, B. C. Interpretation of Optoelectronic Transient and Charge Extraction Measurements in Dye-Sensitized Solar Cells. *Adv. Mater.* **2013**, *25*, 1881−1922.

(23) Hawks, S. A.; Deledalle, F.; Yao, J.; Rebois, D. G.; Li, G.; Nelson, J.; Yang, Y.; Kirchartz, T.; Durrant, J. R. Relating Recombination, Density of States, and Device Performance in an Efficient Polymer:Fullerene Organic Solar Cell Blend. *Adv. Energy Mater.* **2013**, *3*, 1201−1209.

(24) Cotella, G.; Baker, J.; Worsley, D.; De Rossi, F.; Pleydell-Pearce, C.; Carnie, M.; Watson, T. One-Step Deposition by Slot-Die Coating of Mixed Lead Halide Perovskite for Photovoltaic Applications. *Sol. Energy Mater. Sol. Cells* **2017**, *159*, 362−369.

(25) Carnie, M. J.; Charbonneau, C.; Davies, M. L.; Regan, B. O.; Worsley, D. A.; Watson, T. M. Performance Enhancement of Solution Processed Perovskite Solar Cells Incorporating Functionalized Silica Nanoparticles. *J. Mater. Chem. A* **2014**, *2*, 17077−17084.

(26) Troughton, J.; Carnie, M. J.; Davies, M. L.; Charbonneau, C.; Jewell, E.; Worsley, D. A.; Watson, T. M. Photonic Flash-Annealing of Lead Halide Perovskite Solar Cells in 1 ms. *J. Mater. Chem. A* **2016**, *4*, 3471−3476.

(27) O'Regan, B. C.; Barnes, P. R. F.; Li, X.; Law, C.; Palomares, E.; Marin-Beloqui, J. M. Optoelectronic Studies of Methylammonium

Lead Iodide Perovskite Solar Cells with Mesoporous TiO_2: Separation of Electronic and Chemical Charge Storage, Understanding Two Recombination Lifetimes, and the Evolution of Band Offsets during J−V Hyst. *J. Am. Chem. Soc.* **2015**, *137*, 5087−5099.

(28) Pockett, A.; Eperon, G. E.; Peltola, T.; Snaith, H. J.; Walker, A.; Peter, L. M.; Cameron, P. J. Characterization of Planar Lead Halide Perovskite Solar Cells by Impedance Spectroscopy, Open-Circuit Photovoltage Decay, and Intensity-Modulated Photovoltage/Photocurrent Spectroscopy. *J. Phys. Chem. C* **2015**, *119*, 3456−3465.

(29) Gonzalez-Pedro, V.; Juarez-Perez, E. J.; Arsyad, W.-S.; Barea, E. M.; Fabregat-Santiago, F.; Mora-Sero, I.; Bisquert, J. General Working Principles of $CH_3NH_3PbX_3$ Perovskite Solar Cells. *Nano Lett.* **2014**, *14*, 888−893.

(30) Guillén, E.; Ramos, F. J.; Anta, J. A.; Ahmad, S. Elucidating Transport-Recombination Mechanisms in Perovskite Solar Cells by Small-Perturbation Techniques. *J. Phys. Chem. C* **2014**, *118*, 22913−22922.

(31) Contreras, L.; Idigoras, J.; Todinova, A.; Salado, M.; Kazim, S.; Ahmad, S.; Anta, J. A. Specific Cation Interactions as the Cause of Slow Dynamics and Hysteresis in Dye and Perovskite Solar Cells: A Small-Perturbation Study. *Phys. Chem. Chem. Phys.* **2016**, *18*, 31033−31042.

(32) Baumann, A.; Tvingstedt, K.; Heiber, M. C.; Väth, S.; Momblona, C.; Bolink, H. J.; Dyakonov, V. Persistent Photovoltage in Methylammonium Lead Iodide Perovskite Solar Cells. *APL Mater.* **2014**, *2*, 081501.

(33) Gottesman, R.; Lopez-Varo, P.; Gouda, L.; Jimenez-Tejada, J. A.; Hu, J.; Tirosh, S.; Zaban, A.; Bisquert, J. Dynamic Phenomena at Perovskite/Electron-Selective Contact Interface as Interpreted from Photovoltage Decays. *Chem.* **2016**, *1*, 776−789.

(34) Hu, J.; Gottesman, R.; Gouda, L.; Kama, A.; Priel, M.; Tirosh, S.; Bisquert, J.; Zaban, A. Photovoltage Behavior in Perovskite Solar Cells under Light-Soaking Showing Photoinduced Interfacial Changes. *ACS Energy Lett.* **2017**, *2*, 950−956.

(35) O'Kane, S. E. J.; Richardson, G.; Pockett, A.; Niemann, R. G.; Cave, J. M.; Sakai, N.; Eperon, G. E.; Snaith, H. J.; Foster, J. M.; Cameron, P. J.; et al. Measurement and Modelling of Dark Current Decay Transients in Perovskite Solar Cells. *J. Mater. Chem. C* **2017**, *5*, 452−462.

(36) Calado, P.; Telford, A. M.; Bryant, D.; Li, X.; Nelson, J.; O'Regan, B. C.; Barnes, P. R. F. Evidence for Ion Migration in Hybrid Perovskite Solar Cells with Minimal Hysteresis. *Nat. Commun.* **2016**, *7*, 13831.

(37) Bryant, D.; Wheeler, S.; O'Regan, B. C.; Watson, T.; Barnes, P. R. F.; Worsley, D.; Durrant, J. Observable Hysteresis at Low Temperature in "Hysteresis Free" Organic−Inorganic Lead Halide Perovskite Solar Cells. *J. Phys. Chem. Lett.* **2015**, *6*, 3190−3194.

(38) Montcada, N. F.; Marín-Beloqui, J. M.; Cambarau, W.; Jiménez-López, J.; Cabau, L.; Cho, K. T.; Nazeeruddin, M. K.; Palomares, E. Analysis of Photoinduced Carrier Recombination Kinetics in Flat and Mesoporous Lead Perovskite Solar Cells. *ACS Energy Lett.* **2017**, *2*, 182−187.

(39) McMeekin, D. P.; Sadoughi, G.; Rehman, W.; Eperon, G. E.; Saliba, M.; Horantner, M. T.; Haghighirad, A.; Sakai, N.; Korte, L.; Rech, B.; et al. A Mixed-Cation Lead Mixed-Halide Perovskite Absorber for Tandem Solar Cells. *Science* **2016**, *351*, 151−155.

(40) Contreras-Bernal, L.; Salado, M.; Todinova, A.; Calio, L.; Ahmad, S.; Idígoras, J.; Anta, J. A. Origin and Whereabouts of Recombination in Perovskite Solar Cells. *J. Phys. Chem. C* **2017**, *121*, 9705−9713.

(41) Leong, W. L.; Ooi, Z.-E.; Sabba, D.; Yi, C.; Zakeeruddin, S. M.; Graetzel, M.; Gordon, J. M.; Katz, E. A.; Mathews, N. Identifying Fundamental Limitations in Halide Perovskite Solar Cells. *Adv. Mater.* **2016**, *28*, 2439−2445.

(42) Correa-Baena, J.-P.; Turren-Cruz, S.-H.; Tress, W.; Hagfeldt, A.; Aranda, C.; Shooshtari, L.; Bisquert, J.; Guerrero, A. Changes from Bulk to Surface Recombination Mechanisms between Pristine and Cycled Perovskite Solar Cells. *ACS Energy Lett.* **2017**, *2*, 681−688.

(43) Li, Y.; Yan, W.; Li, Y.; Wang, S.; Wang, W.; Bian, Z.; Xiao, L.; Gong, Q. Direct Observation of Long Electron-Hole Diffusion Distance in $CH_3NH_3PbI_3$ Perovskite Thin Film. *Sci. Rep.* **2015**, *5*, 14485.

(44) Meloni, S.; Moehl, T.; Tress, W.; Franckevičius, M.; Saliba, M.; Lee, Y. H.; Gao, P.; Nazeeruddin, M. K.; Zakeeruddin, S. M.; Rothlisberger, U.; et al. Ionic Polarization-Induced Current−Voltage Hysteresis in $CH_3NH_3PbX_3$ Perovskite Solar Cells. *Nat. Commun.* **2016**, *7*, 10334.

(45) Shao, Y.; Fang, Y.; Li, T.; Wang, Q.; Dong, Q.; Deng, Y.; Yuan, Y.; Wei, H.; Wang, M.; Gruverman, A.; et al. Grain Boundary Dominated Ion Migration in Polycrystalline Organic-Inorganic Halide Perovskite Films. *Energy Environ. Sci.* **2016**, *9*, 1752−1759.

(46) Asaduzzaman, A. M.; Schreckenbach, G. Computational Studies on the Interactions among Redox Couples, Additives and TiO_2: Implications for Dye-Sensitized Solar Cells. *Phys. Chem. Chem. Phys.* **2010**, *12*, 14609−14618.

(47) Jennings, J. R.; Wang, Q. Influence of Lithium Ion Concentration on Electron Injection, Transport, and Recombination in Dye-Sensitized Solar Cells. *J. Phys. Chem. C* **2010**, *114*, 1715−1724.

(48) Yang, Y.; Yang, M.; Moore, D. T.; Yan, Y.; Miller, E. M.; Zhu, K.; Beard, M. C. Top and Bottom Surfaces Limit Carrier Lifetime in Lead Iodide Perovskite Films. *Nat. Energy* **2017**, *2*, 16207.

(49) Sherkar, T. S.; Momblona, C.; Gil-Escrig, L.; Bolink, H. J.; Koster, L. J. A. Improving Perovskite Solar Cells: Insights From a Validated Device Model. *Adv. Energy Mater.* **2017**, 1602432.

(50) Xu, J.; Buin, A.; Ip, A. H.; Li, W.; Voznyy, O.; Comin, R.; Yuan, M.; Jeon, S.; Ning, Z.; McDowell, J. J.; et al. Perovskite−fullerene Hybrid Materials Suppress Hysteresis in Planar Diodes. *Nat. Commun.* **2015**, *6*, 7081.